USGS Award Number G09AP00141
Project Duration: 9/1/2009 – 8/31/2010

Final Technical Report

Detection and Location of Non-volcanic Tremor in the New Madrid Seismic Zone

Heather R. DeShon[1], Charles A. Langston[1], Stephen P. Horton[1], Mitch Withers[1]

[1]Center for Earthquake Research and Information
University of Memphis
3876 Central Ave., Suite 1
Memphis, TN 38152-3050

(901) 678-1527, fax (901) 678-4734, hdeshon@memphis.edu
(901) 678-4869, fax (901) 678-4734, clangstn@memphis.edu
(901) 678-4896, fax (901) 678-4734, shorton@memphis.edu
(901) 678-4940, fax (901) 678-4734, mwithers@memphis.edu

Submitted on March 31, 2011

Abstract

Data from the existing Cooperative New Madrid Seismic Network and from a 1-year deployment of a high-frequency phased array are being used to detect and locate non-volcanic tremor (NVT) recently discovered in the New Madrid Seismic Zone (NMSZ). We hypothesize that NVT consists of temporally-energetic swarms of micro-earthquakes at the M_L -1 to -2 level occurring at mid-crustal levels in the NMSZ. Such events were serendipitously detected in November 2006 on a reflection/refraction experiment near the Reelfoot fault where hundreds of small events occurred in one afternoon. Due to its similarity to volcanic tremor, NVT in other environments has been associated with temporal variability in frictional and fluid-related processes. Microearthquake swarm activity along the NMSZ suggest that this intraplate system may also maintain spatial and/or temporal variability of fluid-related processes.

A high-frequency, phased array of 19 broadband seismic stations was deployed beginning in November 2009 over the Reelfoot fault to detect NVT signals at ground motion levels equivalent to M_L -2. Array analysis increases signal-to-noise ratios and yields wave azimuth and slowness information that can be used to estimate locations for these small events. We also set up a network archiving protocol for the existing seismic network to record and process data from selected high-quality stations continuously over the time period of this project. The continuous network data was used to investigate temporal changes in background noise levels that might be due to increased NVT activity at depth. The temporal and spatial characteristics of NVT within the New Madrid fault system are critical parameters that potentially relate a seismic observable to strain within the fault zone. NVT occurring at deep levels in this intraplate fault zone may be related to ductile processes similar to those postulated for NVT in subduction zones and at deep levels of the San Andreas fault. NVT within shallower parts of the fault where typical microseismicity now occurs may reflect unusual brittle failure processes associated with stress heterogeneity or anomalous pore pressure states. Here, we present year 1 data from the array and report on initial findings. The array will be deployed until November 2011 under continuation funding from the USGS [award G11AP20005] and final findings will be reported in association with the technical report for that award in 2011.

Introduction

One of the most exciting discoveries to be made within the New Madrid Seismic Zone (NMSZ) in recent years is the possibility that non-volcanic tremor may be occurring within this intraplate fault system (*Langston et al.*, 2010). A reflection/refraction experiment near Mooring, TN, recorded a sequence of high frequency signals that moved across the linear array at 3-25 km/s. The arrivals were not large enough to trigger the regional seismic network, and continuous seismic data were not archived from nearby stations. The signals could not be well located, but we note that the Mooring experiment was located above the downdip edge of microseismicity associated with the Reelfoot reverse fault. The signals recorded at the Mooring experiment were reminiscent of the packets of energy reported for non-volcanic tremor in subduction and strike-slip fault environments. We use the term "NVT" to represent a continuum of signals ranging from swarms of small overlapping or distinct earthquakes lasting days to noise-like tremor lasting minutes to days.

NVT is a relatively new phenomenon in fault dynamics that was originally coined to describe coherent noise or tremor signals related to subduction processes in southwest Japan (*Obara*, 2002). The signal has since been found to be associated with episodic slip recorded by GPS in the Cascadia subduction zone of the Pacific Northwest (*Rogers and Dragert*, 2003; *Dragert, et al., 2001*). Improved continuous seismic and GPS data has led to the identification of NVT and/or slow slip processes in subduction zones along Cascadia, Japan, New Zealand, Mexico, and Costa Rica (e.g., *Schwartz and Rokosky*, 2007), Taiwan (*Peng and Chao*, 2008), and at deep levels of the San Andreas fault in central California (e.g., *Nadeau and Dolenc*, 2005; *Shelly,* 2010). Frictional stability arguments would suggest that the transition from stick-slip (velocity strengthening) to aseismic (velocity weakening) may pass through the conditional stability regime in a fairly heterogeneous fashion (e.g., *Scholz*, 1998). Models of tremor based on rate-and-state friction indicate that tremor may arise as seismogenic zone boundary phenomena in the presence of fluids (*Liu and Rice*, 2005; 2007), and, as such, NVT may not be limited to plate boundary faults. Recent studies show that tremor can be modulated by teleseismic and tidal signals (*Nakata et al.*, 2008; *Rubenstein et al.*, 2007, 2008; *Peng et al.*, 2008, 2009; *Ghosh et al.*, 2009) and in some cases is composed of overlapping shear failures (*Shelly et al.*, 2006; *Brown et al.*, 2008, *Maceira et al.*, 2010). NVT may represent failure of critically stressed faults with near lithostatic pore fluid pressures (*Thomas et al.*, 2009).

Our target for this project is to re-identify and find the spatial and temporal location of NVT and other seismic signals, such as swarms, that have been identified within the NMSZ. Our hypothesis is that intense swarms of very small micro-earthquakes ($M_L < 1$) occur regularly within the NMSZ and are associated with strain processes on shallow and deep boundaries of the seismogenic segments of New Madrid faults. We targeted the Reelfoot Fault, the central reverse fault associated with the NMSZ. There are two major data collection tasks: (1) the installation and data collection

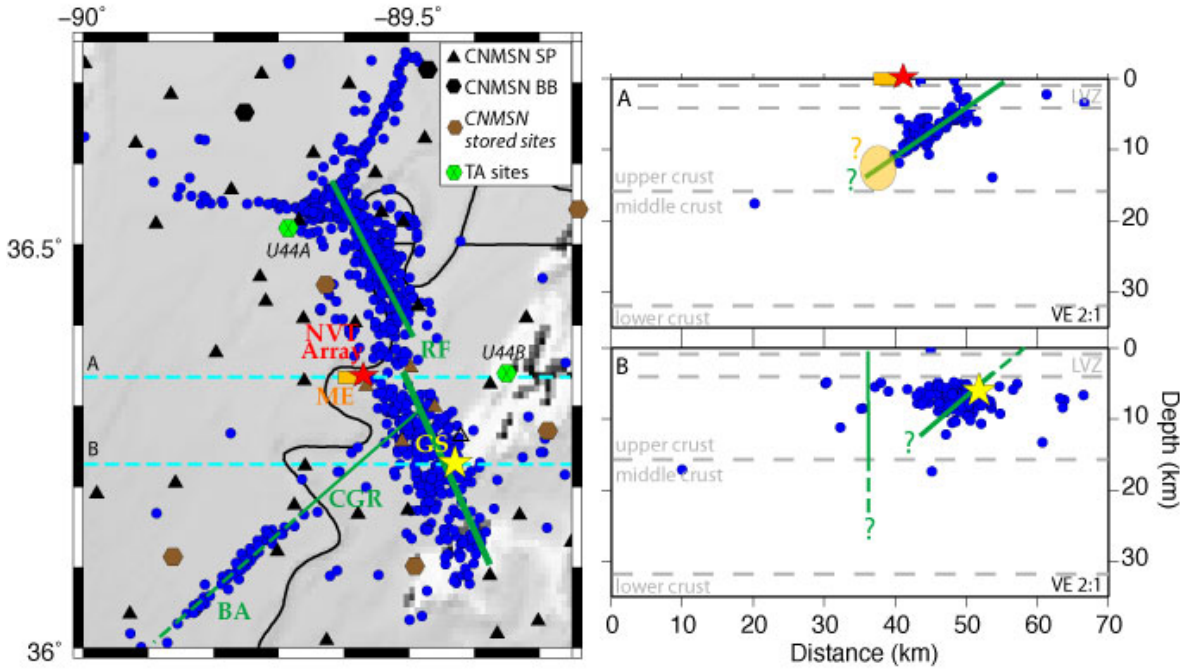

Figure 1 - (left) Map of the New Madrid Seismic Zone. Microseismicity delineates four primary structures including the Reelfoot reverse fault (RF) and the Cottonwood Grove/Blytheville Arch lineation (CGR/BA). Seismicity is recorded by short-period and broadband stations (black triangles and hexagons) associated with the Cooperative New Madrid Seismic Network (CNMSN). Stations being stored in continuous mode as part of this experiment are shown in brown. Red star: current phased site; Orange rectangle: The Mooring experiment; Yellow star: Gratio swarm region; Green hexagons: permit submitted EarthScope Transportable Array sites. Dotted cyan lines show cross-section locations shown at the right. (right) Cross-sections are taken through the NVT array and Mooring Experiment (A) and the Gratio swarms (B). The orange ellipses represent the hypothesized location for signals recorded by the Mooring experiment based on moveout curves.

associated with the phased array and (2) reprogramming of permanent network data protocols to allow for continuous data storage. A 19-station phased array was deployed in November 2009 using instrumentation from the IRIS PASSCAL Instrument Center (Fig. 1, red star). The array was constructed and located to detect high phase velocity P and S waves from the NVT. The array will remain in place until November 2011, assuming seismometers area not re-tasked by PASSCAL due to scheduling conflicts. Data from nine short-period and broadband Cooperative New Madrid seismic network stations (Fig. 1, brown hexagons) are being continuously stored, processed using tremor detection algorithms developed for subduction zone NVT studies, and used to identify and relocate local earthquakes recorded on the array. Results are discussed below.

The NVT Array

NVT is a basic observation that can help understand the dynamics of a fault zone. Tremor sources are difficult to locate because they generally do not have distinct P and S wave arrivals (*Wech and Creager,* 2007). Although tremor sources can be approximately located using envelope time-distance moveout across a network for major peaks in the time series, small aperture, phased arrays offer a superior way to detect and provide far more precise locations of deep non-volcanic tremor. A phased array is capable of directly measuring the phase velocity of the wavefield at any moment in time through conventional plane wave slowness analysis. The measured slowness vectors can be used to constrain event locations (e.g. *Pavlis et al.*, 2004; or *Eagar et al.*, 2006). The 19-element phased array was constructed and located to detect high phase velocity P and S waves from the NVT. Using a phased array significantly increases signal-to-noise levels and provides horizontal slowness and azimuth estimates to locate the source of NVT.

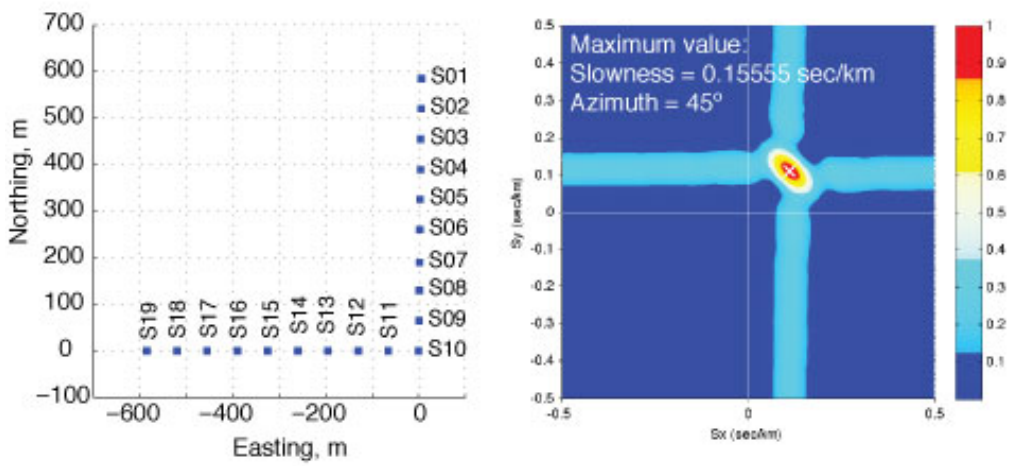

Figure 2 - (left) Geometry of the high-frequency, phased array installed near Mooring, TN. The 19 element array is arranged in an L-shape to take advantage of the available field. (right) Theoretical broadband frequency/wavenumber response for a plane wave with a slowness of 1/6 sec/km, an azimuth of arrival of 45º, and bandwidth between 10-20 Hz. The "L" geometry of the array causes the peak to be elongated in the NW/SE direction with some elongated sidelobes in the NS and EW directions.

The NMSZ is located under an extensive blanket of thick (up to 1 km) unconsolidated sediments of late Cretaceous, Tertiary, and Quaternary age. These sediments represent a challenge for clear recording of microearthquakes and NVT. These sediments cover a complex and deformed Paleozoic section of possibly 7 km deep rift basins of the Reelfoot rift (*Dart and Swolfs*, 1998; *Ervin and McGinnis*, 1975; *Stearns*, 1957; *Stearns and Marcher*, 1962; *Thomas*, 2006). The Paleozoic basement/ sediment interface creates large S-to-P converted phases that can be misidentified as S waves (e.g., *Andrews, et al.*, 1985; *Langston*, 2003). Thus, 3-component recording is a must to discriminate between P and S waves. Sediments of the embayment also amplify ambient ground motions compared to sites on more

competent rock outside of the embayment (*Jemberie and Langston*, 2005) and also act as an efficient high frequency waveguide that can produce high amplitude body and surface waves (*Langston et al.*, 2005; 2006). Increased noise levels also tend to mask signals from small events. Array recording is necessary to increase signal-to-noise ratios for natural seismicity and to discriminate and identify seismic phases on the basis of their horizontal phase velocities and particle motions. The combination of relative P and S arrival times, azimuth and horizontal slowness measurements enables an estimate of the location of events.

ARRAY DESIGN AND RESPONSE

The 19-station high-frequency, phased array is presently deployed in northwestern Tennessee in the region of the Mooring Experiment (Fig. 1, Table 1). It was difficult to find large, unused fields in the vicinity of the Reelfoot Fault to install an areally-distributed array. The natural geometry was to use the edge of a large farm field to site array elements in order to cut down on land usage costs and improve the logistics of installation and servicing at the expense of a somewhat degraded array response (Fig. 2). The array is being used to search for coherent tremor signals propagating across the array and greatly improves signal to noise ratio for very small events. Figure 2 shows the current array geometry and the theoretical broadband f-k response (10-20 Hz) for a wave arriving at 45 degrees azimuth with a phase velocity of 6 km/s. The required "L" geometry of the array causes the peak to be elongated in the NW/SE direction with some elongated sidelobes in the NS and EW directions.

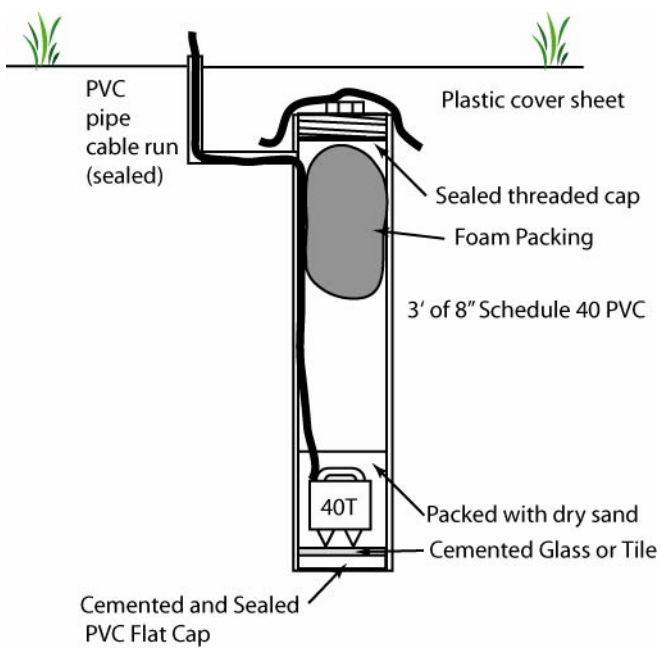

Figure 3: Schematic station installation design. Each sensor is placed in a 4 ft mini-borehole, packed with dry sand, and insulated.

We installed PASSCAL equipment consisting of CMG-40T seismometers, Reftek-130 DAS's, and solar panels (Fig. 3). Continuous data are collected from flash drives in the field every ~8-16 weeks, quality controlled, and sent to the IRIS Data Management Center for archiving. Data from station S10 are made available at this time, while the remaining 18 stations remain under 2-year proprietary usage. All data covering the report period (Nov. 2009 – Oct. 2011) will be archived with the DMC under network code Y8 (Fig. 4). CMG-40T sensors were the appropriate choice here for three reasons. First, they are less subject to the long experimental delays in requests for sensors with a wider recording bandwidth. Second, the bandwidth of this sensor is more than adequate for this experiment (10 or 30 s to 100 Hz). Finally, the noise level in this area is high enough that higher sensor noise level is not a factor. Maintenance has been minimal, and data quality very high. End stations S01, S18, and S19 lost data during the extreme regional flooding event of May 2010 (Julian days 122-202). All sensor and data acquisition changes are correctly recorded in metadata at the DMC. Table 1 lists the station locations.

Table 1: Station Locations

Station	Latitude	Longitude	Elevation(km)	Easting(m)*	Northing(m)*
S01	36.3190	-89.5326	0.089	0	540
S02	36.3184	-89.5327	0.087	0	480
S03	36.3178	-89.5327	0.087	0	420
S04	36.3173	-89.5327	0.088	0	360
S05	36.3166	-89.5327	0.088	0	300
S06	36.3160	-89.5327	0.088	0	240
S07	36.3154	-89.5327	0.087	0	180
S08	36.3149	-89.5328	0.088	0	120
S09	36.3143	-89.5328	0.087	0	60
S10	36.3137	-89.5328	0.087	0	0
S11	36.3137	-89.5335	0.088	-60	0
S12	36.3137	-89.5343	0.087	-120	0
S13	36.3137	-89.5350	0.087	-180	0
S14	36.3137	-89.5357	0.087	-240	0
S15	36.3137	-89.5364	0.088	-300	0
S16	36.3138	-89.5371	0.088	-360	0
S17	36.3138	-89.5379	0.087	-420	0
S18	36.3138	-89.5386	0.086	-480	0
S19	36.3138	-89.5393	0.087	-540	0
GLST	36.2692	-89.2877	0.122		
LEPT	36.2985	-89.4607	0.066		
MORT	36.3247	-89.5662	0.083		
WYBT	36.3477	-89.4975	0.082		
RDGT	36.2562	-89.5110	0.081		
HICK	36.5408	-89.2288	0.141		
LNXT	36.1013	-89.4913	0.144		
PEBM	36.1132	-89.8623	0.076		
PENM	36.4502	-89.6280	0.085		

*Array stations approximate to center station S10.

Permanent Network Data

Continuous recordings for nine CNMSN broadband and short-period stations located near the NVT array have been stored under this award (Fig. 1, Table 1). Storage required the completed installation and testing of CNMSN upgrades to data transfer protocols and a creation of an experiment specific waveserver at the network communication node LNXT. Once in place, we were able to begin storage of continuous data in the form of miniseed day volumes (Fig. 4). Technical problems with the new data transfer protocols and our automated storage scripts contributed to a significant loss of stored data for this experiment in mid-2010. These problems have since been overcome, as evidenced by the improved data recovery shown in Fig. 4b. Storage of broadband data (HICK, LNXT, PENM, PEBM, and WYBT) has been more consistent then the short-period data (GLST, LEPT, MORT, RDGT).

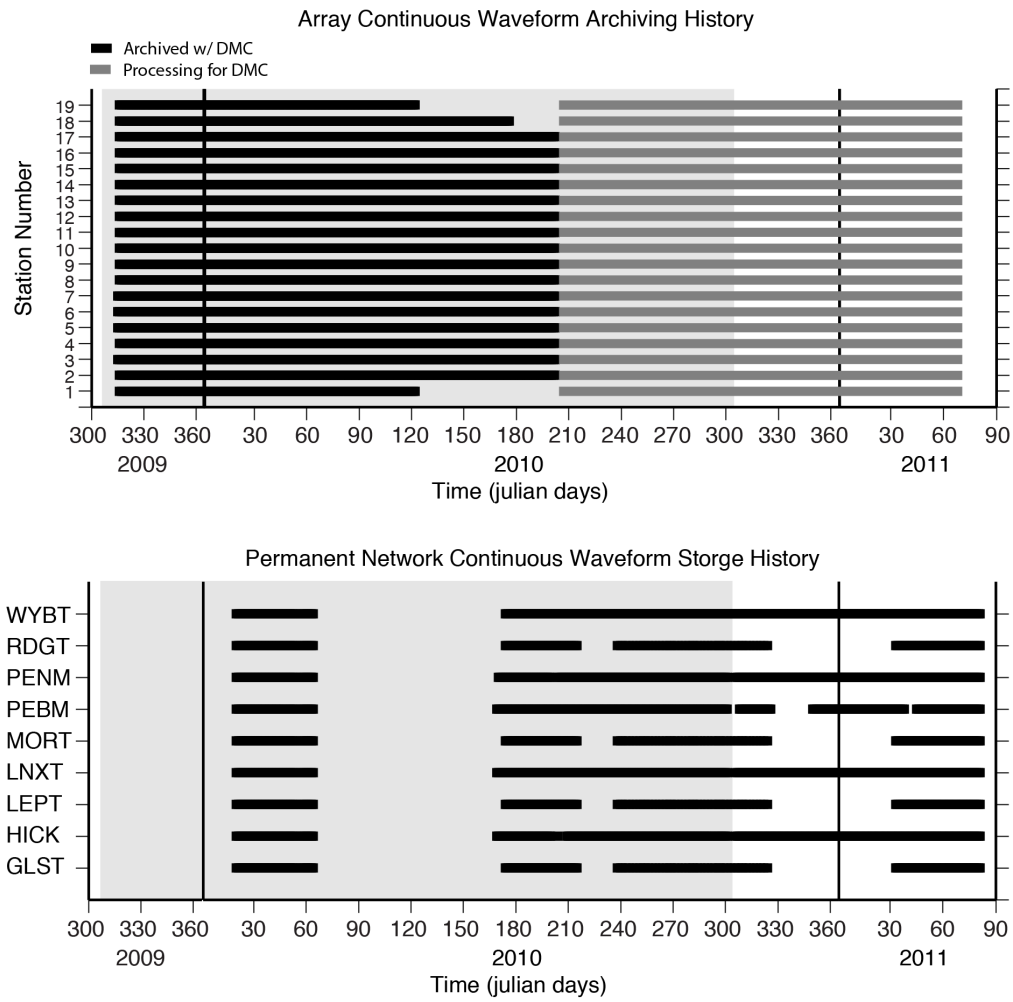

Figure 4: Data archive and storage history for the NVT array continuous data and selected permanent network stations. The gray shading shows the project period covered by this report.

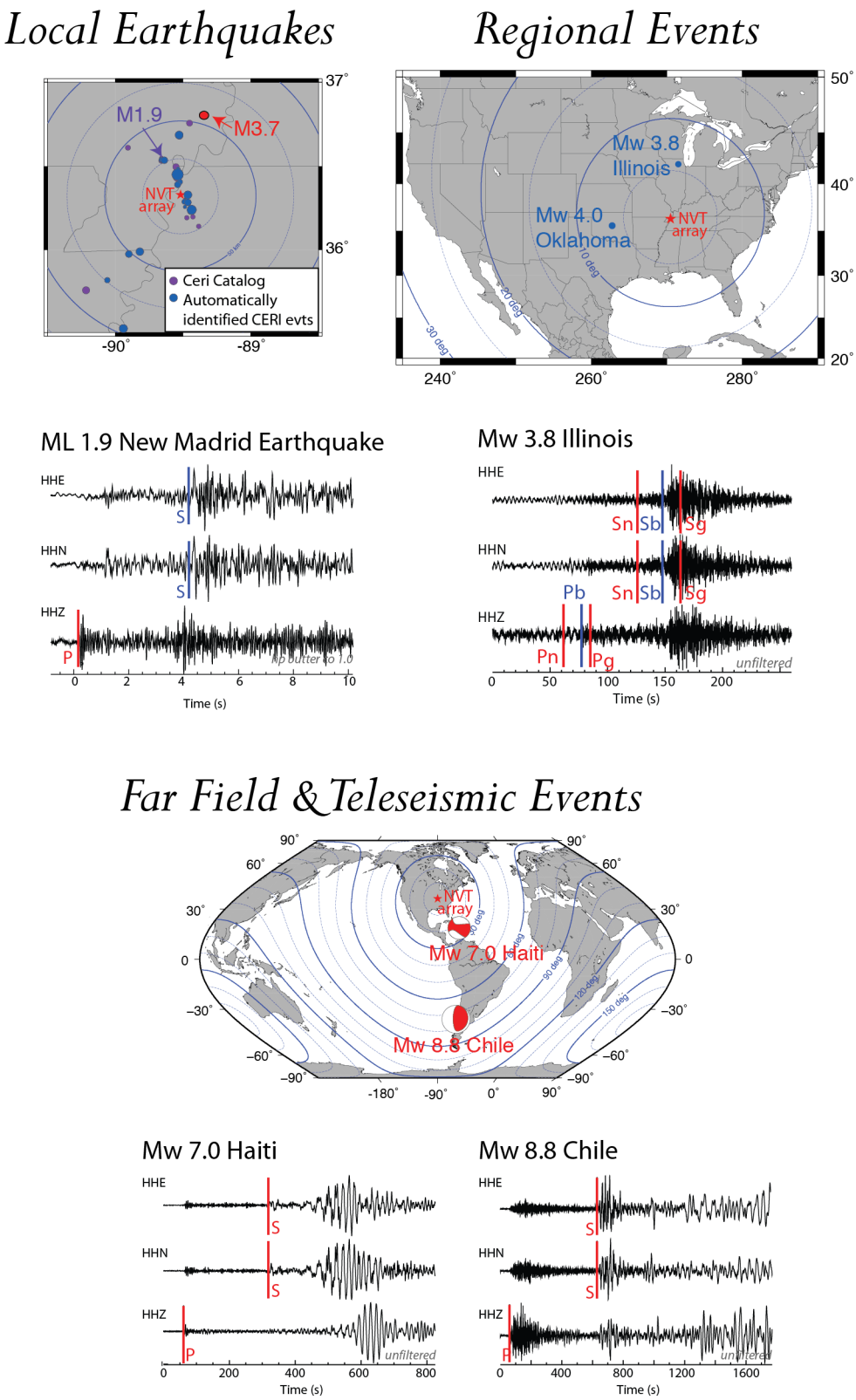

Figure 5. Example waveforms from station S10 of local, regional, far field and teleseismic earthquakes recorded by the NVT array. Data quality is excellent.

Array and limited permanent network data are integrated into an Antelope database, which allows for automatically detecting arrivals and associating local earthquakes to the CERI catalog. We appear to be identifying local earthquakes at a slightly higher rate than the CNMSN event catalog, though of course our automated location ability is severely limited by the single array and small number of reporting stations using standard location methods. The array and network has already recorded many significant earthquakes and seismic signals (Fig. 5), which could be used for allied studies. Teleseismic events include the Mw 7.0 Haiti, Mw 8.8 Maule Chile, and Mw 9.0 Tohoku-Oki earthquakes; regional events in Oklahoma and northern Illinois have also been recorded. The array also recorded a series of airgun shots along the Mississippi River in summer 2010. The array data combined with the continuous CNMSN waveforms and pick catalog will be an excellent dataset for a range of local earthquake studies and it may prove useful to look for triggered seismicity along the Reelfoot Fault. Triggered microseismicity and triggered tremor have been reported along the San Andreas Fault (e.g., *Peng et al.*, 2008,2009; *Thomas et al.*, 2009), and we continue to explore the possibility that either microseismicity or NVT signals could be triggered in the NMSZ.

Continuous networks recordings are additionally being monitored for tremor using the Brudzinski and Allen (2007) method. Continuous data is bandpass filtered between 2-8 Hz, a Hilbert transform applied to calculate an envelope function, daytime hours are removed (05:45-18:45 CST), earthquakes are removed, and then daily median nighttime amplitude is calculated. For broadband data stored in 2009, we saw correlation in the time series at multiple stations at low amplitudes with mean wind velocities recorded at nearby weather stations. Analysis of continuous data collected under this award is ongoing.

Significant Results

ABILITY TO RESOLVE SMALL SIGNALS

Currently we are using the BroadBand frequency/wavenumber (BBFK) analysis of *Nawab et al.* (1985) to analyze the array data without any corrections for individual array element site structures. Figure 6 shows the BBFK result for 20 s of low-amplitude, oscillatory signal that is comparable in amplitude to signals seen in the discovery data of possible non-volcanic tremor from the Reelfoot Fault in 2006. This demonstrates that the array will be sensitive enough to detect similar possible NVT in the future. However, the character of the present signal is quite different, showing periodic behavior and oscillatory motions. The array response shows two main sources of these waves to the NW and to the North. The apparent velocity is approximately 2 km/s and is consistent with the sediment-trapped P wave that is the dominant high-frequency phase seen in explosion data (*Langston et al.*, 2005). This noise source is likely from farm machinery or pumping and consists of acoustic waves propagating in the unconsolidated sediments of the embayment. The configuration and sensitivity of the array is sufficient to detect signals of the size seen in the discovery data set.

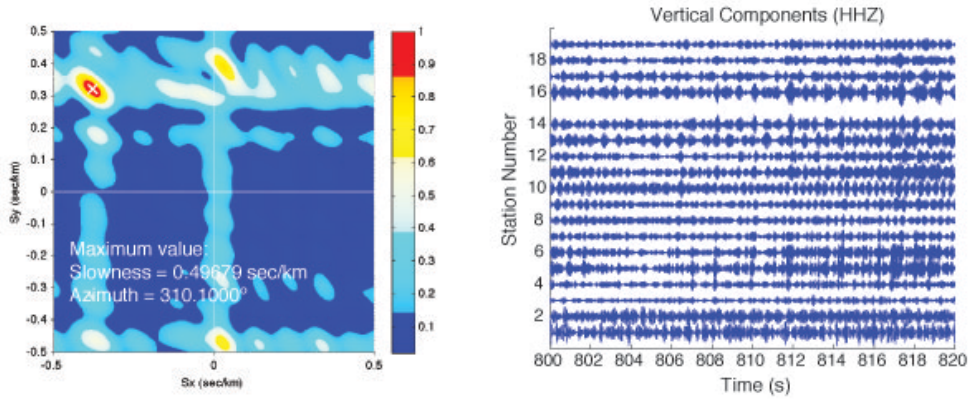

Figure 6 - (left) Frequency/wavenumber response for background noise filtered between 10-20 Hz. (right) Plot of the filtered background noise used for BBFK analysis. An oscillatory, ambient noise signal was detected. These signal levels are comparable to those seen in the discovery data of possible non-volcanic tremor from the Reelfoot Fault in 2006 and demonstrate that the array will be sensitive enough to detect similar possible NVT in the future.

However, the array responses for the observed signals (Fig. 7) show the effect of multipathing that produces the irregular character of the side-lobes compared to the theoretical response shown in Figure 2. Analysis of P and S wave signals from small local earthquakes (not shown) also demonstrate that waves are not purely coherent at these high frequencies across the array. It is likely that the near-surface layer, which is about 10 m thick in this area (*Langston*, 2003), is variable across the array and that array deconvolution techniques (e.g., *Der et al.*, 1987) will be used to improve the array response over the course of continuation funding.

BROADBAND FK ANALYSIS OF A LOCAL EARTHQUAKE

We have conducted BBFK analysis on a M3.7 earthquake recorded by the array (See Figure 5 for location). The waveforms are typical for NMSZ earthquakes, showing a large Sp conversion on the vertical component generated at the base of the unconsolidated sediment-basement interface, here about 700m under the array (Fig. 7). The extremely low velocity of near-surface material is evident from the lack of P wave motion on the horizontal components. The expected azimuth to the source based on the network location is 17º. BBFK results for the P waveforms indicated that the array response maximum is over 30º away from the expected azimuth (Fig. 7, top). The response also shows considerable multipathing. These waves can be seen in the moveout of various wavelets behind direct P in the data. The source of multipath arrivals is likely due to variations in the velocity structure of the upper few meters across the array. For NS S-waves, the wavefield is much more complicated, and array response shows considerable evidence of multipath S-wave arrivals (Fig. 7, bottom). Low-pass filtering the EW S-wave data shows a remarkable succession of S wave reverberations in the sediment column.

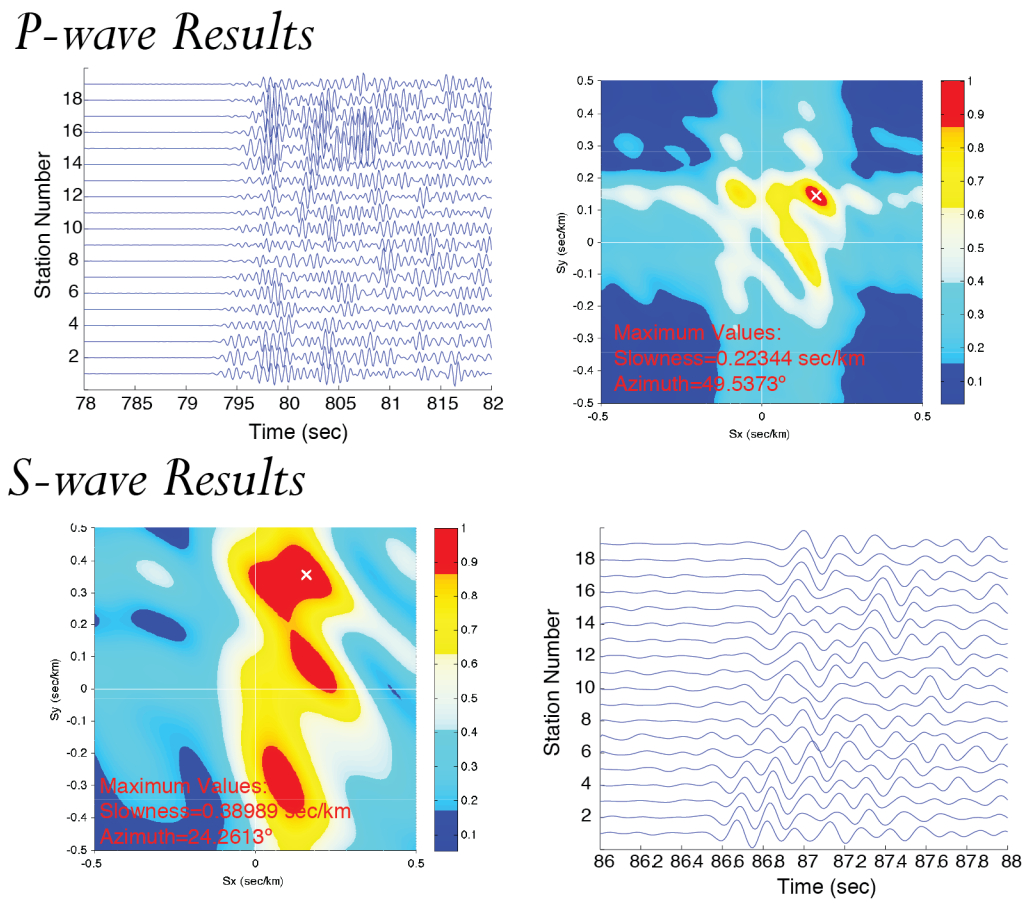

Figure 7: (top) BBFK results (right) using filtered P waveforms (left) for the M3.7 earthquake. (bottom) BBFK results (left) using filtered NS S waveforms (right).

AUTOMATED PROCESSING OF ARRAY DATA

We have investigated a number of techniques to pick out possible NVT from background noise using the character of the array response from local earthquakes and the character of the events seen in the discovery data set. Events seen in the discovery data set had high apparent velocities that were greater than 3km/s and phase move-outs that indicated a source region to the west. They were also best seen in the 8-15 Hz frequency band. Thus, we are looking for similar high frequency arrivals in the array data set. It becomes important to examine the array response to incident P and S waves from local earthquakes, as done above, and to have some knowledge of the ambient seismic noise field.

A straightforward way of approaching this problem is to examine short, consecutive 6 sec array beams and look at the distribution of azimuth and slowness for the largest peak in the beam within the 8-15 Hz frequency band. This simple analysis shows that much of the ambient noise comes from low velocity (high slowness) waves that come from near-surface sources. Indeed, a plot of peak azimuth vs. time shows that there are strong cultural noise sources, interpreted to be trains, that

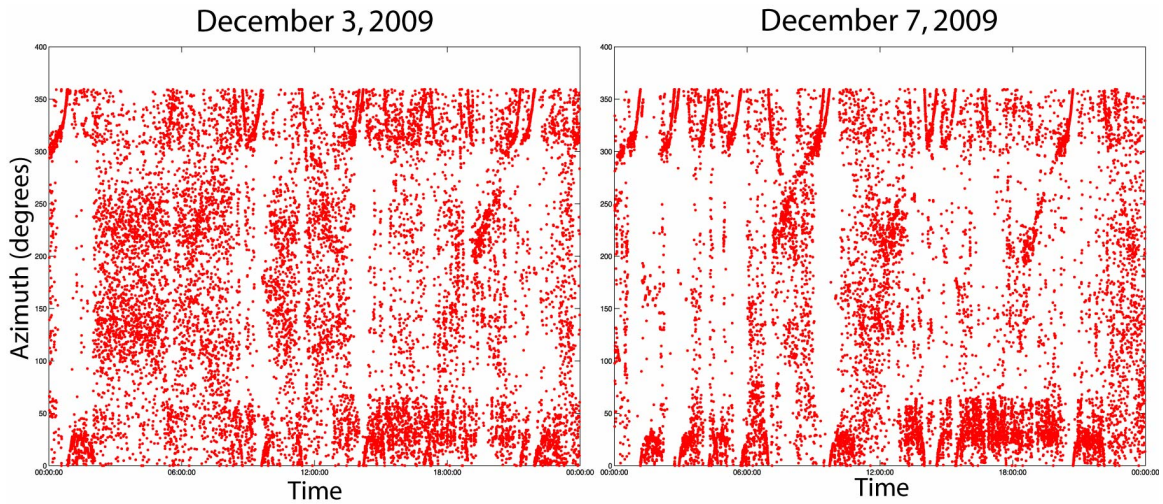

Figure 8: Azimuth of peak energy in the 8-15 Hz frequency band plotted as a function of time for 2 days of array data. Streaks of noise are seen that consistently occur as sources that move from north-to-south or south-to-north. These are interpreted to be trains on a track 5 km to the east.

occur throughout the data and produce large, slowly propagating surface waves (Fig. 8).

Analysis of the first month of data collected by the array yielded a small number of very low magnitude events with high phase velocity but no anomalous swarms were seen consistent with the discovery data set. We are trying other algorithms that include a combination of frequency-wave number analysis with time domain beams so we can quantify time domain noise levels and observed high-velocity events.

The array is working well and because of our ability to analyze signals at very low ground motion levels comparable to the discovery data set, we are confident that we will be able to detect and identify similar signals if and when they reoccur.

Indirect Support of Undergraduate Interns

Two IRIS (Incorporated Research Institutions in Seismology) undergraduate interns were indirectly supported by this award. Funding support for the interns comes directly from IRIS, but both students' research efforts were directly applicable to the goals of this USGS award. Sarah Wiley worked with H. DeShon over the summer of 2009 and into fall 2009 on noise analysis of permanent network sites. She presented results at the 2009 Fall Meeting of the American Geophysical Union. Blaine Bockholt worked with C. Langston over the summer of 2010 performing beam-forming calculations on the 19-station NVT array data. He also aided S. Horton with servicing runs of the array over that time period. His results were presented at the 2010 Fall Meeting of the American Geophysical Union.

Award Bibliography to Date

Wiley, S., H.R. DeShon, O.S. Boyd (2009). Seismic Noise Characterization in the Northern Mississippi Embayment, *Eos Trans. AGU, 90(52)*, 2009 Fall Meet. Suppl., Abstract S23A-1730.

Langston, C.A., H.R. DeShon, S. Horton, and M. Withers (2010), Preliminary Results for the Detection of Non-volcanic Tremor in the New Madrid Seismic Zone, 2010 Spring Meeting, SSA, *Seismo. Res. Letts.*, 81(2), 379.

Bockholt, B., C.A. Langston, H.R. DeShon, S. Horton (2010), The Search for Non-volcanic Tremor on the Reelfoot Fault, Northern Tennessee, Abstract S23A-2094 presented at the 2010 Fall Meeting, AGU, San Francisco, Calif., 13-17 Dec.

References Cited

Andrews, M. C., W. D. Mooney, and R. P. Meyer (1985). The relocation of microearthquakes in the northern Mississippi embayment, *Jour. Geophys. Res.*, *90*, 10223-10236.

Brown, J., G. Beroza, D. Shelly (2008), An autocorrelation method to detect low frequency earthquakes within tremor, *Geophys. Res. Letts.*, 35, L16305, doi:10.1029/2008GL034560.

Brudzinski, M. R., and R. M. Allen (2007). Segmentation in episodic tremor and slip all along Cascadia, *Geology, 35*, 907-910, doi:10.1130/G23740A.1

Dart, R. L., and H. S. Swolfs (1998). Contour mapping of relic structures in the Precambrian basement of the Reelfoot rift, North American midcontinent, *Tectonics*, *17*, 235-249.

Der, Z. A., R. Shumway, and A. Les (1987). Multi-channel deconvolution of *P* waves at seismic arrays, *Bull. Seism. Soc. Am.* **77,** 195–211.

Dragert, H., K. Wang, and T. S. James (2001). A silent slip event on the deeper Cascadia subduction interface, *Science*, *292*, 1525-1528.

Eagar, K. C., G. L. Pavlis, and M. W. Hamburger (2006). Evidence of possible induced seismicity in the Wabash Valley Seismic Zone from improved microearthquake locations, *Bull. Seism. Soc. Amer*, 96, 1718-1728, doi:10.1785/0120050190.

Ervin, C. P., and L. D. McGinnis (1975). Reelfoot rift: Reactivated pre- cursor to the Mississippi embayment, *Geol. Soc. Am. Bull.*, *86*, 1,287-281,295.

Forte, A. M., J. X. Mitrovica, R. Moucha, N. A. Simmons, and S. P. Grand (2007). Descent of the ancient Farallon slab drives localized mantle flow below the New Madrid seismic zone, *Geophys. Res. Lett.*, *34*, doi:10.1029/2006GL027895.

Ghosh A, Vidale JE, Peng ZG, et al. (2009), Complex nonvolcanic tremor near Parkfield, California, triggered by the great 2004 Sumatra earthquake, *J. Geophys. Res.*, 114, B00A15.

Jemberie, A.L., and C.A. Langston (2005). Site Amplification, scattering and intrinsic attenuation in the Mississippi embayment from coda waves, *Bull. Seism. Soc. Am., 95,* 1716-1730.

Langston, C. A. (2003). Local Earthquake Wave Propagation Through Mississippi Embayment Sediments: I. Body Wave Phases and Local Site Responses, *Bull. Seism. Soc. Am.*, *93*, 2664-2684.

Langston, C.A. D.M. Rieger, and M.B. Magnani (2010), Unusual Microseisms Seen in the Reelfoot Fault Zone, Northern Tennessee, from a Reflection Experiment, *Bull. Seism. Soc. Am.*, 100, 377-383.

Langston, C. A., P. Bodin, C. Powell, M. Withers, S. Horton, and W. Mooney (2005). Bulk sediment Qp and Qs in the Mississippi embayment, Central U.S., *Bull. Seism. Soc. Am.*, *95*, 2162-2179.

Langston, C. A., P. Bodin, C. Powell, M. Withers, S. Horton, and W. Mooney (2006). Explosion source strong ground motions in the Mississippi embayment, *Bull. Seism. Soc. Am.*, *96*, 1038-1054.

Liu, Y., and J. R. Rice (2005), Aseismic slip transients emerge spontaneously in three-dimensional rate and state modeling of subduction earthquake sequences, *J. Geophys. Res.*, 110, B08307, doi:10.1029/2004JB003424.

Liu, Y.J. and J.R. Rice (2007), Spontaneous and triggered aseismic deformation transients in a Subduction fault model, *J. Geophys. Res.*, 112, B09404, doi:10.1029/2007JB004930.

Maceira M, Rowe CA, Beroza G, et al. (2010), Identification of low-frequency earthquakes in non-volcanic tremor using the subspace detector method, *Geophys. Res. Letts.*, 37, L06303.

Nadeau, R. M., and D. Dolenc (2005). Nonvolcanic tremors deep beneath the San Andreas Fault, *Science*, *307*, 389.

Nakata R, Suda N, Tsuruoka H (2008), Non-volcanic tremor resulting from the combined effect of Earth tides and slow slip events, *Nature Geosci.*, 1, 676-678.

Obara, K. (2002). Nonvolcanic deep tremor associated with subduction in southwest Japan, *Science*, *296*, 1679.

Pavlis, G. L., F. L. Vernon, D. Harvey, and D. Quinlan (2004). The generalized earthquake location (GENLOC) package: A modern earthquake location library, *Computers in Geosciences,* 30, 1079-1091.

Peng ZG, Chao KV (2008), Non-volcanic tremor beneath the Central Range in Taiwan triggered by the 2001 M-w 7.8 Kunlun earthquake, *Geophys. J. Int.*, 175, 825-829.

Peng ZG, Vidale JE, Creager KC, et al. (2008), Strong tremor near Parkfield, CA, excited by the 2002 Denali Fault earthquake, *Geophys. Res. Letts.*, 35, L23305.

Peng ZG, Vidale JE, Wech AG, et al., (2009), Remote triggering of tremor along the San Andreas Fault in central California, *J. Geophsy. Res.*, 114, B00A06.

Rogers, G., and H. Dragert (2003). Episodic tremor and slip on the Cascadia subduction zone: the chatter of silent slip, *Science*, *300*, 1942-1943.

Rubinstein JL, Vidale JE, Gomberg J, et al. (2007), Non-volcanic tremor driven by large transient shear stresses, *Nature*, 448, 579-582.

Rubinstein JL, La Rocca M, Vidale JE, et al. (2008), Tidal modulation of nonvolcanic tremor, *Science*, 319, 186-189.

Scholz, C.H. (1998), Earthquakes and friction laws, *Nature*, *391*, 37-42.

Schwartz, S. Y., and J. M. Rokosky (2007), Slow slip events and seismic tremor at circum-pacific subduction zones, *Rev. Geophys*., 45, RG3004, doi:10.1029/2006RG000208.

Shelly DR, (2010), Migrating tremors illuminate complex deformation beneath the seismogenic San Andreas fault, *Nature*, 463, 648-U75.

Shelly, D. R., G. C. Beroza, S. Ide, and S. Nakamula (2006), Lowfrequency earthquakes in Shikoku, Japan and their relationship to episodic tremor and slip, *Nature*, 442, 188–191.

Stearns, R. G. (1957). Cretaceous, Paleocene, and lower Eocene geologic history of the northern Mississippi embayment, *Geol. Soc. Am. Bull.*, *68*, 1077-1100.

Stearns, R. G., and M. V. Marcher (1962). Late Cretaceous and subsequent structural development of the northern Mississippi embayment area, *Geol. Soc. Am. Bull.*, *73*, 1387-1394.

Thomas, W. A. (2006). Tectonic inheritance at a continental margin, *GSA Today*, *16*, doi: 10.1130/1052-5173.

Thomas AM, Nadeau RM, Burgmann R (2009), Tremor-tide correlations and near-lithostatic pore pressure on the deep San Andreas fault, *Nature*, 462, 1048-U105.
Wech, A. G., and K. C. Creager (2007). Cascadia tremor polarization evidence for plate interface slip, Geophys. Res. Let., 34, L22306, doi:10.1029/2007GL031167.